Ultrasound in Med. & Biol., Vol. 2, pp. 279–285. Pergamon Press, 1976. Printed in Great Britain.

TWO DIMENSIONAL ULTRASOUND SCANNING OF EXCISED BRAINS—I. NORMAL ANATOMY

R. F. HEIMBURGER*†, F. J. FRY*, T. D. FRANKLIN*, N. T. SANGHVI*, G. GARDNER* and J. MULLER‡

(*First received* 6 *January* 1976; *and in final form* 26 *January* 1976)

Abstract—This study demonstrated techniques for visualization of detailed brain anatomy with two dimensional ultrasound. The use of large aperture focused ultrasound transceivers appears to be essential for displaying the outlines of thalamus, internal capsule and substantial nigra in addition to those of the ventricles. The ability to vary grey scale and edge enhancement using either linear or logarithmic amplification through a scan converter assisted in identification of anatomical structural detail. It was most clearly visualized when the images were displayed with accentuation of edge enhancement. Brain position during ultrasound scanning was also important for maximal visualization of structural detail.

Anatomical studies are useful in clinical application of two dimensional ultrasound brain visualization, to assure maximum diagnostic information with minimum scan time. The development of ultrasound diagnostic instruments and techniques is expected to add valuable information to computer assisted tomography, isotope brain scanning and cerebral angiography in the management of brain disorders, particularly in infants.

Key words: Ultrasound brain visualization, Normal excised brain, Thalamus, Internal capsule, Substantia nigra, Cerebral ventricles, Third ventricle.

INTRODUCTION

Dussik's hope of visualizing the brain when he initiated diagnostic ultrasound in 1942 has been slow in development. Instrumentation and techniques for two dimensional brain visualization, although promising, have not been clinically accepted or widely utilized. White *et al.* (1967) enumerated the problems of using small aperture unfocused ultrasound transceivers, with relatively inflexible display systems, because of an inability to penetrate the adult skull. In 1970 Fry *et al.*, using a large aperture focused ultrasound transceiver, demonstrated the ability to visualize grey–white interfaces in normal brains through the intact, healed scalp of living patients, after a large skull section had been removed. Heimburger *et al.* (1973) extended this observation to identify the internal capsule and the substantia nigra. In 1972 Kossoff and Garrett reported visualization of intracranial structures of fetuses *in utero*. An ultrasound brain atlas of the normal infant was published in 1974 by Kossoff *et al.* It showed considerable anatomical detail. McCrae (1975) and White (1975) questioned the ability of Kossoff *et al.* (1974) to identify the structures they claimed to visualize. White (1975) suggested that scanning isolated brains could determine whether deep grey-matter structures can actually be demonstrated with two dimension visualization equipment.

Advance in diagnostic ultrasound instrumentation made by the authors of this report (1970, 1973, 1975, 1976), by Kossoff (1972, 1974) and by Somer (reported by Freund *et al.*, 1973) has provided new hope for the clinical acceptance of two dimensional ultrasound brain visualization. The rapid development and acceptance of computer assisted X-ray tomography, suggests that ultrasound investigators seek areas that provide diagnostic services which are not and probably cannot be made available to computer assisted X-ray tomography. Not to detract from the significant contribution this radiological development has made to brain diagnosis, the one thing it lacks, and probably will continue to lack, is portability. Ultrasound instrumentation can be made portable to provide diagnostic services to critically ill patients included recent head injury victims (Heimburger *et al.*, 1975, 1976). The ability to demonstrate structural detail in the infant brain with ultrasound instrumentation reported by Kossoff *et al.* (1974) and Heimburger *et al.* (1976), combined with the desire to avoid ionizing irradiation, favor ultrasound for brain diagnosis in infants. Ultrasound diagnostic testing, using non-invasive, non-accumulative beams, has not added to the risk of critical head injured patients as a result of its use in echoencephalography over the past 20 yr. It may decrease the time required to diagnose and evacuate intracranial hematomas (Heimburger, 1976). Accurate diagnosis of brain damage in neonatal infants is expected to be particularly benefitted (Heimburger *et al.*, 1976).

Two dimensional ultrasound visualization of excised brains was initiated by the authors in 1969 primarily to confirm the observation that abnormal appearing reflections within the brain, arise from grossly visible tumor. This work was reported in 1973 by Heimburger *et al.* To further the possible effectiveness of using portable two dimensional ultrasound diagnostic instrumentation for neonatal infants, as well as for head injured children and adults, a study of normal excised brains has been undertaken.

Available scan time in the brain injured is brief because

For reprints contact R. F. Heimburger, M. D., Neurological Surgery, Indiana University Medical Center, Indianapolis, IN 46202, U.S.A.

*From Fortune-Fry Research Laboratory of the Indianapolis Center for Advanced Research, Indiana University School of Medicine.

†From the Department of Surgery, Neurological Surgery, Indiana University School of Medicine.

‡From the Department of Pathology, Neuropathology, Indiana University School of Medicine.

Supported in part by The Fortune Behest and by NINDS Grant No. 5R01NS 10983-03RAD.

of physical condition and restlessness. Exploratory scanning for orientation and identification of structure must be done rapidly to provide maximum information in the shortest possible time. To organize clinical ultrasound scan routines, it appeared advisable to obtain data regarding ultrasound equipment, transceiver geometry, scanning modes, gain parameters, display configuration, head positioning and coupling. Two dimensional ultrasound scanning of excised brains with and without pathology, covered or uncovered by meninges, skull bone, scalp and hair should be undertaken to provide as much information as possible to guide clinical application, as well as continued instrument development. No previous report of two dimensional ultrasound scanning of excised brains has been found in the medical literature.

This report will be limited to two dimensional ultrasound scanning of normal excised brain without covering. Brain positioning to maximize visualization of normal internal anatomy will be demonstrated, as it relates to clinical application in living patients.

METHOD

Prototype ultrasound scanning equipment designed for clinical application was used in this study. Lead metaniobate transceivers, ground spherically to focus at 10–20 cm, were passed in a simple linear path through a tank of degassed water over the immersed formalin fixed brains. A two dimensional picture was displayed on a 17-in. monitor for quick recognition. Permanent records were made on polaroid film from either of two separate 9-in. monitors. One of the 9-in monitors displayed a duplicate of the image on the 17-in. screen. They were in line with a scan converter which permitted either logarithmic or linear amplification to provide different degrees of edge enhancement and grey scale display. The second 9-in. monitor had no grey scale capability, to determine the value of edge enhancement when used alone.

The formalin fixed brains were first washed in tap water and then immersed in a tank of degassed water. Air was carefully removed from ventricles, sulci and subarachnoid spaces. This required many hours of immersion with occasional turning and gentle manipulation. Poor scan quality indicated that some air remained trapped, and additional mainpulation was needed.

The brains were meticulously positioned so that the focal point of the ultrasound beam fell on the midline, anteriorly and posteriorly, as well as superiorly and inferiorly. This was facilitated by having an indication of the focal point sweep visible on the display monitor, (see Fig. 1, Scan *P* 40).

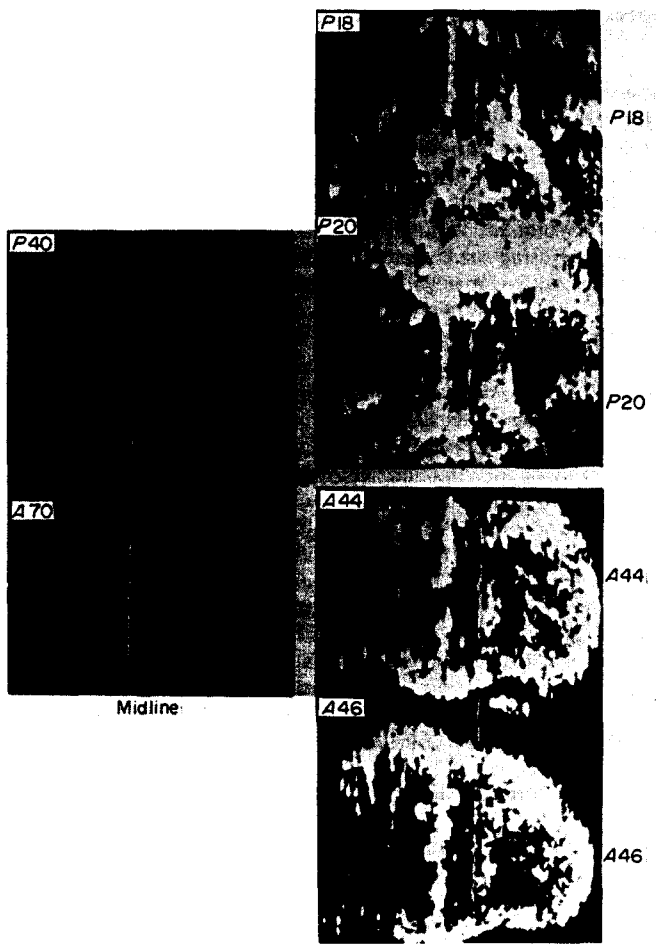

Fig. 1. Coronal ultrasound scans of a normal formalin fix human brain, oriented so that the sweep of the focal point of the ultrasound beam passes directly along the midline. The two scans on the left show the midline posteriorly (*P* 40) and anteriorly (*A* 70) with the thin focal line passing along it. A slight sag of the brain is visible posteriorly. Localization of reference scan planes is illustrated in the four scans on the right. *P* 18 shows a definite small interruption of the midline echo just above the heavy cerebellum reflection. *P* 20, a plane 2 mm posterior to *P* 18, shows an intact midline echo. A similar "break" is demonstrated anteriorly at *A* 44 and *A* 46. These reference planes can be used to reliably select a desired scan plane.

Since transparent overlays from a stereotaxic atlas (Delmas *et al.*, 1959) were used to identify anatomical structures, stereotaxic planes and terminology have been adopted. Each ultrasound scan displays a one millimeter section of brain tissue oriented either horizontally or coronally, depending on the relationship of the scan path to the brain. The primary identification plane was related to the base of the brain. A number of reference points have been used to identify a primary basilar plane, each varying slightly from the others. The orbital surfaces of the frontal lobes correspond closely with a primary basilar plane identified by the midpoint of the external auditory canals bilaterally, and the inferior rims of the orbits bilaterally (Reid's plane). This plane was used to position the brains for both horizontal and coronal ultrasound scans. Horizontal scans were made parallel to the inferior orbital rim, external auditory canal plane in patients, or parallel to the orbital surfaces of the frontal lobes, which is a corresponding basilar plane, in excised brains. Horizontal planes were designated in millimeters, superior or inferior to the basilar plane, i.e. HS60 represents a plane 60 mm superior to the basilar plane while HS-5 lies 5 mm inferior. Coronal scane planes were oriented perpendicular to the basilar plane. The coronal plane that passes through the middle of the external auditory canal was designated as the Ear Bar Zero (EBO) plane. Measurements from it anteriorly (*A*) and posteriorly (*P*) expressed in millimeters accurately locate additional coronal scan planes, i.e. *P* 40 indicates a plane 40 mm posterior to the EBO plane while *A* 70 is 70 mm anterior to EBO (Fig. 1).

The midline structures of the brain were clearly visible in patients, and in the excised brains, both in horizontal and coronal ultrasound scans. The break in the midline, produced by the corpus callosum, was visible superiorly in horizontal scans, and both anteriorly and posteriorly in the coronal scans. The change between a completely intact midline echo pattern and a break in this pattern produced by the corpus callosum occurred abruptly, and could be identified repeatedly in scan planes 1 or 2 mm apart. Reference planes were identified by visualizing these "break points". The most accurate "break point" reference plane occurred 20 mm posterior (*P* 20) to the EBO plane (Fig. 1). In *P* 18 (Fig. 1) the break in the midline echo pattern is barely visible. *P* 20, which is 2 mm posterior to *P* 18, has an intact midline without a break. *P* 20 was found to be the most reproducible reference plane in both patients and excised brains. Less accurately located was the anterior (*A* 40) to EBO. The anterior break was not as predictable at *A* 40, as the posterior break was at *P* 20, but varied several millimeters as demonstrated in Fig. 1 (*A* 44–*A* 46). The horizontal "break" occurred about 60 mm (*HS* 60) above basilar plane; but, due to differences in head shape and contour, was even less predictable in its location, varying as much as a centimeter. These identifying reference planes were readily located in normal brains both *in vivo* and *in vitro*. Edema and other pathological conditions made the "break point" planes less easily visualized ultrasonically. After the formalin fixed brains were accurately located in relationship to the scan planes of the ultrasound instrument, a variety of transceivers and gain settings were used to determine the most effective instrumentation for anatomical structure visualization and identification. For this study a large aperture transceiver (1.7 MHz 5 cm dia. lead metaniobate, spherically ground to focus at 20 cm) provided the clearest anatomical structure visualization. A simple linear scan mode was used, mechanically passing the transceiver over the brain in either horizontal or coronal paths. Gain attenuation was added or subtracted to optimize visualization. Displays using the amplification systems—linear and logarithmic—both related to a scan converter, were compared with an amplification system providing maximum edge enhancement (Fig. 2).

The excised brains were placed on a platform that could accurately angulate or rotate the midline plane of the brain in relationship to the transceiver sweep. Measurable changes in brain position were carried out to determine whether visualization of anatomical structural detail would be improved or diminished. The sweep of the transceiver's focal point was displayed as a line on the monitor screens. Relationship of brain midline angulation to the transceiver sweep was identified and either corrected, or accurately measured. Rotation around the long axis of the brain was not as easily detected in the ultrasound scans, but did provide a visible effect on the image (Fig. 6).

RESULTS

Figure 1 illustrates the ability to quickly line up the sweep of the ultrasound focal point with the midline of the brain (*P* 40 and *A* 70). Scanning for brain midline alignment in relationship to the focal point sweep demonstrated a very slight sag of the brain, anteriorly and posteriorly, from its mid-section where it is supported (Fig. 1, *P* 40 and *A* 70). Identification of the splenium of the corpus callosum is made through visualization of the "break point" in the continuum of the midline at *P* 18 as compared to *P* 20 in Fig. 1. A similar "break" in the midline continuity by the genu of the corpus callosum is also seen anteriorly between *A* 44 and *A* 46. The anterior "break point" plane may vary as much as 4 to 5 mm from *A* 40. The posterior "break point" plane is more reliable at *P* 20–*P* 18 in living patients, as well as in excised brains.

The three display possibilities available to the instrument are illustrated in Fig. 2. Maximum grey scale display using logarithmic amplification is illustrated in the top row of scans. Linear amplification, with lesser grey scale and some increase in edge enhancement, is present in the middle row. Maximum edge enhancement without grey scale, is shown in the lower row. Comparable gain settings are displayed in each row, highest decibel attenuation on the left, lowest on the right. Although the accurate one to one magnification, displayed in the lower row of scans, was convenient for direct measurement and brain atlas overlay studies, recognition of familiar anatomical structure is improved when the entire coronal section of the brain is displayed.

Grey scale in the upper row of Fig. 2. was pleasing to view, but the edge enhancement of the two lower rows displays the outlines of the thalamus on both right and left sides more distinctly. This is particularly true in the lower row, where greatest edge enhancement has been achieved. Attempts to visualize the internal capsule were not as successful in the excised brains as in patient visualization, possibly because the internal capsule is narrowed by formalin fixation, making resolution of its medial and lateral borders more difficult.

The cerebral ventricles are collapsed and very difficult to visualize ultrasonically in excised, normal brains. It is probable that pulsation and blood flow around the ventricular ependyma makes the walls of these cavities more reflective of ultrasound during life. In Fig. 2 the ventricles are best visualized as small clear areas just above the "heart shaped" thalamus in the upper row of scans. The left lateral ventricle, closer to the ultrasound transceiver,

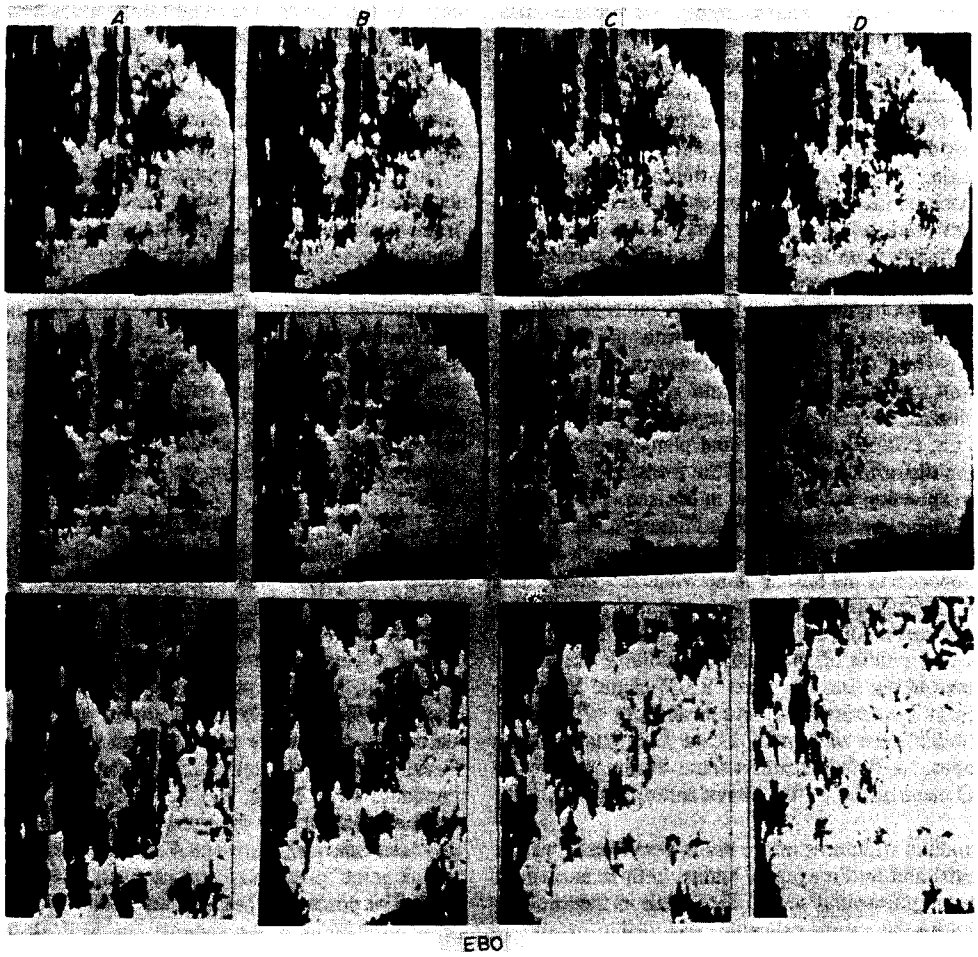

Fig. 2. Each of the 12 coronal scans was made at Ear Bar Zero (EBO). The upper row of scans was made with logarithmic amplification for maximal grey scale. Linear amplification combining grey scale with edge enhancement was used for the middle row. Maximal edge enhancement without grey scale was used for the lower row of scans. The upper two rows were made at $\frac{1}{2}$:1 magnification. The lower row was made at 1:1 magnification. Gain was increased comparably for each display made from left to right. The heart shaped thalamus–internal capsule interfaces are recognized in each of the scans. The scan beam entering the brain from the right side displays the border of the left thalamus more clearly due to attenuation of the ultrasound beam by passage through tissue. The edge enhancement displayed in the lower row increases the visibility of the thalamic borders. The lateral ventricles are outlined, adjacent to the midline superior to the thalamus, most clearly in the upper two rows under *B*. The inferior border of the lateral ventricle, adjacent to the thalamus, produces a heavy reflectance. The two walls of the third ventricle could not be resolved. The substantia nigra produces heavy echoes in the inferior portion of the thalamus.

is more discernible than the right one. The inferior walls of the lateral ventricles, forming the superior medial borders of the thalamus bilaterally, provide relatively heavy reflectivity.

The lateral border of the thalamus was most clearly visible at EBO in the coronal scans (Fig. 3). Moving the scan plane 5 mm anterior (*A* 5) or posterior (*P* 5) decreases the reflectance of the interface between the thalamus and external capsule, presumably because the thalamic borders curve away, slightly, anteriorly and posteriorly from EBO.

Moving the sweep of the focal point so that it passes through a particular structure sometimes will increase definition of that structure. This maneuver is illustrated in Fig. 4 in which the sweep of the focal point has been moved 1 and 2 cm to the right (closer to the brain surface) and the same distance to the left of the midline plane (deeper into the brain). The attenuation produced by passage of the sound beam through a greater or lesser thickness of brain tissue alters the pattern of reflection. The interfaces which outline the internal capsule were visualized a little more clearly both on the right and on the left sides of the brain, when the sweep of the focal point passed more nearly through the border of that side of the thalamus. A suggestion of separation of the two walls of the third ventricle in its superior portion was made when the focal sweep was to the right of the midline. The internal capsule is not as clearly outlined in any of these scans as it is in living brains, but there is a suggestion of its resolution particularly on the left side of the brain, in the lower row of scans, using maximum edge enhancement.

Ventricular outlines were particularly difficult to define in excised brains due to collapse of the ventricular space. At the level of the anterior enlargement of the lateral ventricles (*A* 40) in coronal scans, the ventricular outline was made out with linear amplification in the upper two scans (*A* and *B*) on either side of the midline echo (Fig. 5). With logarithmic amplification, to provide more ap-

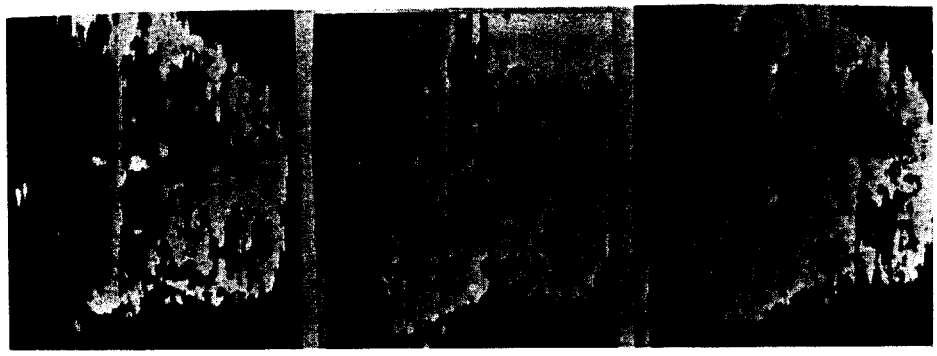

Fig. 3. Coronal scans made at the Ear Bar Zero (EBO) plane and 5 mm anterior (*A* 5) and 5 mm posterior (*P* 5) demonstrate the thalamic border echo best at EBO. The Sylvian fissure and Island of Reil are well displayed on the right side of the *A* 5 scan. The two edges of the internal capsule are best seen at EBO on the left, where the lateral border of the thalamus extends inferiorly to provide the medial internal capsule outline while the heavy globus pallidum echo, provides its lateral edge. The pons is most prominent at EBO inferior to the lower surface of the temporal lobes. The lateral ventricles are poorly demonstrated in these scans. The third ventricle is clearly seen at its greatest superior inferior extent at *A* 5. There is a suggestion of resolution of the two walls of the third ventricle at EBO. The posterior portion of the third ventricle, with its lesser superior–inferior extent, is seen at *P* 5.

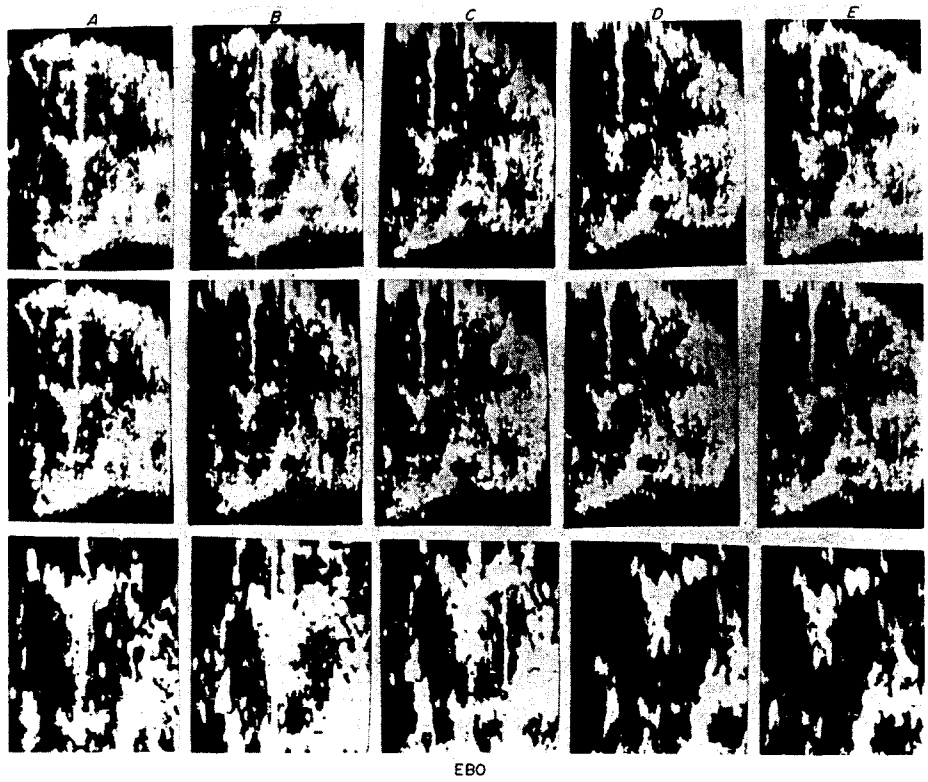

Fig. 4. Fifteen coronal scans made at the Ear Bar Zero (EBO) plane are shown.

Maximal grey scale is shown in the top row of scans and maximal edge enhancement in the lower row, as in Fig. 2.

The sweep of the focal point fell on the midline in the scans under *C*. It swept 1 cm (under *B*) and 2 cm (under *A*) to the left of the midline. The focal point swept 1 cm (under *D*) and 2 cm (under *E*) to the right of the midline. The thalamic border and internal capsule were clearly identified when the focal line passed through them (2 cm from the midline) on either side. This improvement in identification is not sufficiently clear to warrant shifting the focus sweep from the midline in clinical use. Definition of the two walls of the third ventricle changed when the focal line depth was changed. Visualization of the lateral ventricular walls was slightly improved when the focal line passed through them particularly on the right.

propriate dynamic range compression for grey scale display, the two lateral ventricles were also visible in the lower two scans. When the scan converter was set for increased edge enhancement (Fig. 5C) the ventricular outlines were more visible than when grey scale was increased (Fig. 5D). The ventricular outline would probably not have been identified if grey scale alone had been used, indicating that both logarithmic and linear amplification provided important visual cues.

In Fig. 6 the brain was tilted around its longitudinal and

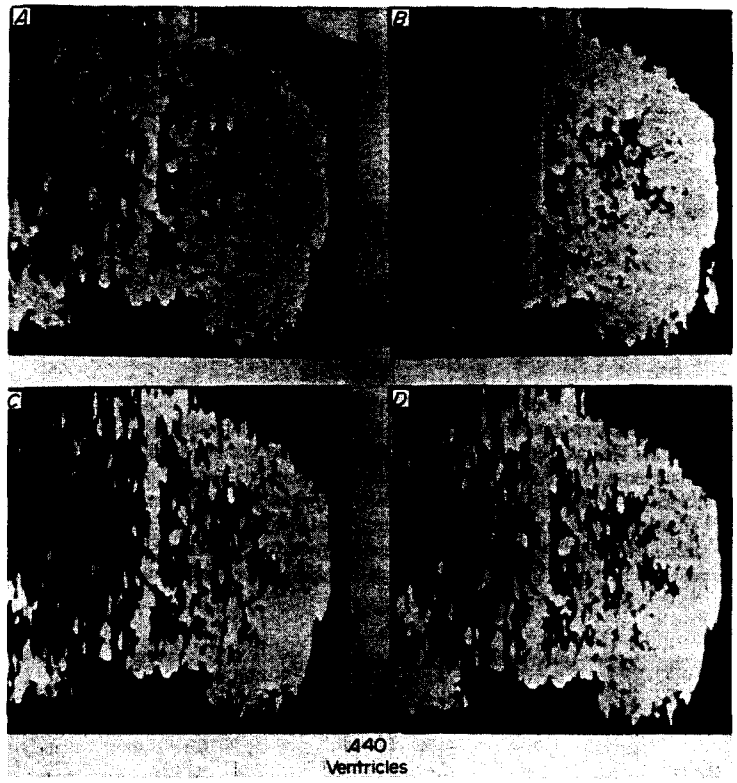

Fig. 5. Four coronal scans of the anterior enlargement of the lateral ventricles at *A* 40 are shown. Scans *A* and *B* made with linear amplification are compared with scans *C* and *D* using logarithmic amplification. The heavy reflecting dot in the middle of each ventricular outline is probably choroid plexus. Ventricular outlines were more easily discerned when linear amplification was used to provide both edge enhancement and grey scale in the display.

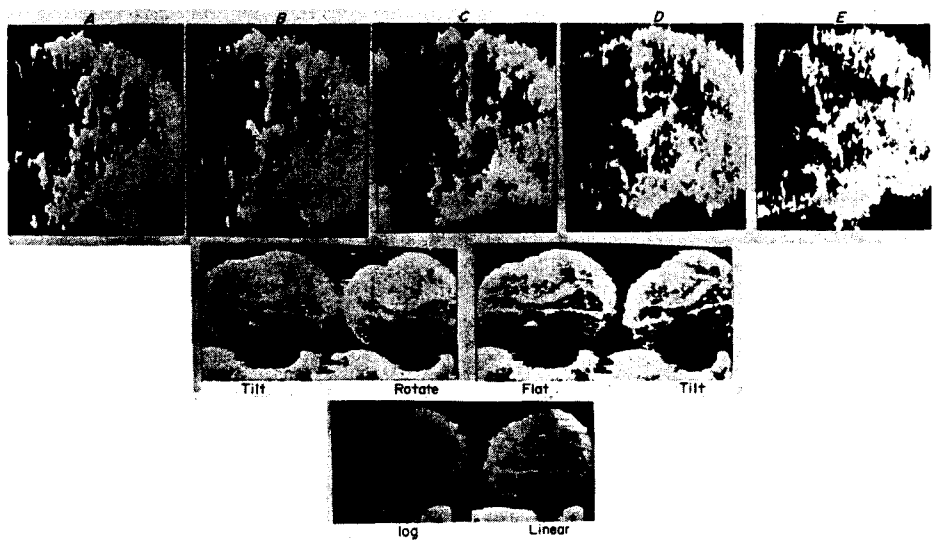

Fig. 6. Five coronal and six horizontal scans are used to illustrate the effect of brain angulation and rotation. Scan *C* in the upper row shows the focal sweep along the brain midline. As the brain is tilted 5° (*B*) and 10° (*A*) to the left and equally to the right (*D* and *E*) some of the thalamus outline is lost. In 10° tilt (scans *A* and *E*) the superior outline of the thalamus is enhanced on the right (closer to the transceiver) but diminished, by the attenuation of passing through more tissue on the left. The right side of the brain is to the right and the vertex superior in each of the coronal scans.

Tilting the brain, in horizontal scan, (anterior up on the left, posterior up on the right in the second row) changed the third ventricle echo slightly, but had little effect on visualization of other structures. When the brain was rotated around its long axis (Rotate) both walls of the third ventricle were clearly visible. In the lower row 2 scans are used to compare linear and log amplification for identifying the walls of the lateral ventricles. Very little difference is shown, except the slanting posterior portion of the right (upper) lateral ventricle is more clearly resolved by linear amplification. In all the horizontal scans the anterior portion of the brain is to the left. The right side of the brain is superior.

coronal axes. The outline of the thalamus in the coronal scans (top row) was not as distinct when the sweep of the focal point was angled 5° or 10°, to either the right or to the left. Only one wall of the third ventricle on the side of angulation became visible when the brain was tilted instead of both walls appearing fused as it was when the focal point sweeps along the midline.

In horizontal scans (Fig. 6 middle row) a few degrees of tilt elevating the anterior (far left) or posterior (far right) portion of the brain did not appear to change the heavy echo from the lateral surface of the lateral ventricle but did alter the reflectance of the walls of the third ventricle. Rotating the brain around its long axis did bring out the two walls of the third ventricle (Fig. 6 Rotate).

Comparison of logarithmic and linear amplification to delineate the lateral walls of the lateral ventricles (lower row, Fig. 6) illustrated the advantages of edge enhancement with linear amplification for identifying structural outlines. The slanting posterior edge of the right lateral ventricle in the linear scan was more easily identified than in the scan using logarithmic amplification.

DISCUSSION

This study demonstrates the ability of ultrasound visualization techniques to identify and display, normal brain anatomy. Apparently some of the interfaces between grey and white matter have a sufficient ultrasound impedence mismatch to reflect ultrasound beams and be displayed. Similar interface displays are also visualized in living brains, (Heimburger *et al.*, 1973). It seems likely that differences in the vasculature of grey and white matter, and the pulsation of the living brain accentuates the impedence mismatch to make the grey–white borders more visible to ultrasound in living brain that in formalin fixed brains. The adult skull still presents a formidable barrier to two dimensional ultrasound brain visualization. Available technology can overcome the skull barrier and provide brain images of clinical value.

Acknowledgements—Mrs. Vera Leslie prepared the manuscript and Joe Deina the illustrations. The authors are grateful.

REFERENCES

Delmas, A., Pertuisett, B. and Pineau, M. H. (1959) *Craniocerebral Topometry in Man.* Mason Cie Editeurs, Paris and Charles C. Thomas, Springfield, IL.

Dussik, K. T. (1942) Über die Möglichkeit hoch frequente mechanische Schwingungen als diagnostiches Hilfsmittel zu ver werten. *Ftschr. ges. Neurol Psychiat.* **174**, 153–168.

Freund, H. J., Kendel, H. K., Kendel, H. K., Kristian and Voigt, K. (1973) Electronic sector scanning in the diagnosis of cerebrovascular disease and space occupying processes. *Neurology* **23**, 1147–1159.

Fry, F. J., Heimburger, R. F., Gibbons, L. V. and Eggleton, R. C. (1970) Ultrasound for visualization and modification of brain tissue. *IEEE J. Sonics Ultrasonics.* **17**, 165–169.

Heimburger, R. F., Eggleton, R. C. and Fry, F. J. (1973) Ultrasonic visualization in determination of tumor growth rate. *J. Am. Mech. Ass.* **224**, 497–501.

Heimburger, R. F., Fry, F. J. and Eggleton, R. C. (1973) Ultrasound visualization in human brain: the internal capsule, a preliminary report. *Surg. Neurol.* **1**, 56–58.

Heimburger, R. F., Fry, F. J., Franklin, T. D. and Eggleton, R. C. (1975) Ultrasound visualization of intracranial hemorrhage. *Ultrasound in Medicine*, Vol. 1, pp. 265–271. Plenum Press, New York.

Heimburger, R. F., Fry, F. J., Franklin, T. D., Jr. and Eggleton, R. C. (1976) Ultrasound diagnosis for head injuries. *J. Indiana State Med. Assoc.* **6**, 247–249.

Kossoff, G. and Garrett, W. J. (1972) Intracranial detail in fetal echograms. *Invest. Radiol.* **7**, 159–163.

Kossoff, G., Garrett, W. J. and Radavanovich, G. (1974) Ultrasonic atlas of normal brain of infant. *Ultrasound Med. & Biol.* **1**, 259–266.

Kossoff, G. (1975) Letters to the Editor (re: ultrasound atlas of normal brain of infant). *Ultrasound Med. & Biol.* 1, 412.

McRae, D. L. (1975) Letters to the Editor (re: ultrasonic atlas of normal brain of infant). *Ultrasound Med. & Biol.* **1**, 411.

White, D. N. *et al.* (1967) Studies in ultrasonic echoencephalography—VII. General principles of recording information in ultrasonic *B*- and *C*-scanning and the effects of scatter, reflection and refraction by cadaver skull on this information. *Med. Biol. Engng* **5**, 3–14.

White, D. N. (1975) Letters to the Editor (re: ultrasonic atlas of normal brain of infant). *Ultrasound Med. & Biol.* **2**, 45–46.